Numerical model of quantum oscillations in quasi-two-dimensional organic metals in high magnetic fields

N. Harrison, R. Bogaerts, and P. H. P. Reinders
Laboratorium voor Vaste-Stoffysica en Magnetisme, Katholieke Universiteit Leuven, Celestijnenlaan 200D, B-3001 Heverlee, Belgium

J. Singleton and S. J. Blundell
Department of Physics, University of Oxford, The Clarendon Laboratory, Parks Road, Oxford, OX1 3PU, United Kingdom

F. Herlach
Laboratorium voor Vaste-Stoffysica en Magnetisme, Katholieke Universiteit Leuven, Celestijnenlaan 200D, B-3001 Heverlee, Belgium
(Received 1 February 1996; revised manuscript received 10 May 1996)

Departures from standard Lifshitz-Kosevich behavior observed in the oscillatory magnetization and magnetoresistance of bis(ethylenedithio)tetrathiafulvalene (BEDT-TTF) charge-transfer salts in high magnetic fields are investigated using a numerical model of the Landau levels in a quasi-two-dimensional metal. The numerical model enables oscillations in the chemical potential to be treated, as well as the effects of finite temperature, Landau level broadening, and the presence of additional quasi-one-dimensional Fermi surface sheets. The numerical calculations reproduce experimental magnetization data successfully, and allow several phenomena observed in the experiments to be investigated. It is found that pinning of the chemical potential to the Landau levels is responsible for the apparent anomalously low effective masses of the higher harmonics of the de Haas–van Alphen oscillations observed in recent experiments. In addition, the quasi-one-dimensional components of the Fermi surface are found to have a pronounced influence on the wave form of the oscillations in the model, providing a means by which their density of states can be estimated from experimental results. Whilst the magnetization is a thermodynamic function of state, calculations of the behavior of the magnetoresistance are much more model dependent. In this paper, recent theoretical models for the longitudinal magnetoresistance in semiconductor superlattices have been modified for use with the BEDT-TTF salts and are shown to successfully reproduce the form of the experimental data. The strongly peaked structure of the magnetoresistance, which comes about when the chemical potential is situated in or close to the gap between adjacent Landau levels, is found to be responsible for the apparent strong increase of the effective mass which has recently been reported in high field transport measurements. [S0163-1829(96)07137-8]

I. INTRODUCTION

The method derived by Lifshitz and Kosevich (LK) has been used to treat quantum oscillatory phenomena such as the Shubnikov–de Haas (SdH) and de Haas–van Alphen (dHvA) effects in metals for many years with great success.[1] Recently, however, quantum oscillations have been observed to depart significantly from conventional LK behavior in a number of charge-transfer salts based on the molecule bis-(ethylenedithio)tetrathiafulvalene (BEDT-TTF).[2–5] These departures become most apparent when the temperature dependence of the oscillations is analyzed in an attempt to determine the quasiparticle effective mass m^*. In particular, the higher harmonics of the oscillations are found to be more weakly dependent on temperature than predicted by the LK model,[1] leading to estimates for m^* which are lower than those derived from the fundamental frequency.[2,3] In the case of the SdH effect, an apparent increase of the effective mass of the fundamental frequency is also observed at high magnetic fields.[3,4]

The departures from LK behavior at high fields appear to be directly related to the low-dimensionality of the BEDT-TTF salts. In order to gain an understanding of the influence of dimensionality on the quantum oscillations, we have used numerical methods to calculate the magnetization and longitudinal magnetoresistance of a quasi-two-dimensional (Q2D) metal. As the relevant experimental data[2–5] involve measurements of the α-phase BEDT-TTF salts, the model Fermi surface used is based on those calculated for this family of compounds; i.e., it consists of a very slightly warped cylinder plus a quasi-one-dimensional (Q1D) open section. The results of the numerical calculations are successful in accounting for many of the departures from LK behavior observed in the BEDT-TTF salts. Furthermore, although the Q1D part of the Fermi surface does not cause quantum oscillations, its associated density of states plays an important role in determining the wave form of the experimental quantum oscillations. [Note that departures from LK behavior have also been observed in TMTSF (Ref. 6) and BEDT-TTF (Refs. 7, 8) charge-transfer salts due to the presence of a spin-density-wave (SDW) ground state; however, effects due to SDW's are beyond the scope of the model and will not be treated in the present paper.]

This paper is organized as follows: Sec. II gives a more detailed introduction to the problem, and Sec. III presents calculations of the oscillatory magnetization. Section IV describes a method for analyzing experimental magnetization data which takes account of the Q2D nature of the BEDT-TTF salts and Sec. V shows calculations of the magnetoresistance. A summary is given in Sec. VI.

II. A QUASI-TWO-DIMENSIONAL METAL IN A MAGNETIC FIELD

BEDT-TTF salts are often referred to as Q2D, since a small overlap of the molecular orbitals between the conducting planes, in what is usually labeled the crystallographic **b** direction, leads to the formation of a weakly dispersed energy band in the reciprocal lattice k_z direction (i.e., perpendicular to the Q2D k_x, k_y planes).[9,10] For the purpose of this discussion, the three-dimensional (3D) dispersion relation for a closed Q2D portion of Fermi surface is modeled by the equation

$$\varepsilon = \frac{\hbar^2 k_x^2}{2m^*} + \frac{\hbar^2 k_y^2}{2m^*} + \frac{W}{2}(1-\cos[k_z b]). \tag{1}$$

It is the finite interplane bandwidth W which causes the warping of the otherwise perfectly 2D Fermi surface. In some materials, such as β-(BEDT-TTF)$_2$I$_3$,[11] the warping of the Fermi surface is thought to have been observed in the quantum oscillations as a beating effect between two similar frequencies F and $F+\Delta F$. These correspond to the minimum and maximum Fermi surface extremal areas respectively; the difference frequency is given by $\Delta F = Wm^*/e\hbar$. In contrast, the α-phase BEDT-TTF salts do not exhibit pronounced beating effects.[2–4,10,12] For this reason, as far as the quantum oscillatory behavior is concerned, these materials are nearly ideally 2D. A small but finite warping of the Fermi surface is, however, known to be present, owing to its manifestation in the form of angle-dependent magnetoresistance oscillations.[8,13]

The inability to resolve the two separate frequencies in the quantum oscillations implies that the difference in area $\Delta A = 2\pi e \Delta F/\hbar$ between the Fermi surface extremal areas is less than the difference in area $\Delta a = 2\pi eB/\hbar$ between adjacent Landau tubes (i.e., $\Delta F/B < 1$, where B is the magnetic induction). Current experimental evidence suggests an upper estimate of $\sim$5 T for ΔF in the α-phase BEDT-TTF salts.[14] Therefore, by applying the high magnetic fields typically available at pulsed field laboratories[2–4] it is possible to achieve the situation where $\Delta F/B \ll 1$.

This near ideal two-dimensionality implies that the Landau level structure in the density of states (DOS) should become clearly resolved. The sharpness of the Landau level structure depends not only on the degree of warping of the Fermi surface, but also on the extent to which the Landau levels are broadened by the finite quasiparticle lifetime τ. Only when the width of the Landau levels $\hbar\tau^{-1}$ is less than the cyclotron energy $\hbar\omega_c$ (where $\omega_c = eB/m^*$) can the Landau levels be well resolved. As a consequence, the size of the oscillatory contribution to the density of states $\tilde{g}[\varepsilon,B]$ becomes comparable to or larger than the field-averaged (background) DOS $\overline{g[\varepsilon]}$. In this situation, where $\tilde{g}[\varepsilon,B] > \overline{g[\varepsilon]}$, the chemical potential μ becomes pinned to the highest occupied Landau tube and therefore oscillates as the magnetic field is swept.[15] We refer to this situation as the ''high magnetic field limit'': in 3D systems, it is reached only in the extreme quantum limit when one Landau tube is occupied.[15] However, for the Q2D systems considered in this paper, the high magnetic field limit is reached when 10 or 20 Landau tubes are still occupied.[2–5]

The conventional LK theory is based on the assumption that μ is constant; as has been described above, this is only a valid approximation in a Q2D system at very low magnetic fields.[1,15] Therefore, in a derivation of the oscillatory magnetization or magnetoresistance of a Q2D system, the full magnetic field and temperature dependence of $\mu[B,T]$ must be taken into account. This involves finding the inverse of the integral

$$N = \int_0^\infty g[\varepsilon,B] f[\varepsilon,\mu]\,\partial\varepsilon \tag{2}$$

over all states. Here, N is the total number of electrons per unit volume, which is held constant, $g[\varepsilon,B] \equiv \tilde{g}[\varepsilon,B] + \overline{g[\varepsilon]}$ is the total DOS, and $f[\varepsilon,\mu] = (1+\exp[(\varepsilon-\mu)/kT])^{-1}$ is the Fermi-Dirac distribution function.

An analytical solution for $\mu[B,T]$ can be found for the extreme case of an ideal 2D electron gas with infinitely sharp Landau levels. This approach was adopted by Vagner *et al.*[16] in an attempt to explain dHvA measurements made on 2D GaAs/Al$_x$Ga$_{1-x}$As heterojunctions and graphite intercalation compounds.[17] The scope of their solution was, however, somewhat limited owing to the fact that it did not include the effects of Landau level broadening. While an approximate solution which considers Landau level broadening in the case where $T=0$ has been considered,[18] there has yet been no complete analytical solution which fully combines both the effects of Landau level broadening and thermal damping. In contrast, one of the major successes of conventional LK theory is that it can be adapted to include many additional physical effects such as Landau level broadening in the form of harmonic damping factors.[1,15,19]

Without a general analytical solution for $\mu[B,T]$ which can include scattering, etc., it is necessary to resort to numerical methods. Although such methods are more time consuming, they enable the effects of Landau level broadening, finite temperatures and so on to be investigated using the model. In the following section we shall begin by calculating the magnetization (i.e., the de Haas–van Alphen effect). The advantage of calculating the magnetization is that it is a thermodynamic function of state and can therefore be related directly to the free energy of an electron gas. In contrast, the calculation of the magnetoresistance (Sec. V) involves many more assumptions about the electronic scattering mechanisms. As the aim of this paper is to model recent high field data ($B > 20$ T), the warping of the Fermi surface will be ignored for the purpose of the magnetization calculations; as has been discussed above, this is not thought to be an important consideration at magnetic fields above 10 T. However, the existence of a finite Fermi surface warping is necessary for the existence of the longitudinal magnetoresistance, and so is reintroduced in Sec. V.

III. THE OSCILLATORY MAGNETIZATION

The magnetization for an ensemble of electrons is given by the partial derivative

$$M[B,T,N] = -\left.\frac{\partial H_F}{\partial B}\right|_{N,T}, \tag{3}$$

where the Helmholtz free energy H_F is related to the thermodynamic potential

$$\Omega = -kT\int_0^\infty g[\varepsilon,B]\ln[1+e^{(\mu-\varepsilon)/kT}]\partial\varepsilon \tag{4}$$

by the relation

$$H_F = \Omega + \mu N. \tag{5}$$

It can be shown analytically[15] that the magnetization is equivalently given by

$$M[B,T,\mu] = -\left.\frac{\partial\Omega}{\partial B}\right|_{\mu,T}. \tag{6}$$

Here, M is a function of μ which is itself a function of magnetic field and temperature.

Whilst there is as yet no clear consensus regarding the exact form of the Landau level broadening in 2D systems, recent detailed torque magnetization measurements performed on GaAs/(Ga,Al)As heterostructures have been able to probe the DOS rather directly. Experimentally, the functional form of the broadening distribution function is indistinguishable from that of a Lorentzian.[20] Such Lorentzian broadening was originally proposed as an appropriate way of taking into account the effects of quasiparticle scattering in metallic systems by Dingle.[19] A further assumption which can be made to simplify the integration procedure is that the field averaged (or equivalently, zero field) DOS $\overline{g}$ is constant. This is generally expected to be true for a 2D parabolic band.[21] In any case, the precise functional form of the DOS when $\varepsilon \ll \mu$ should not have any significant effect on the magnetization when 10–20 Landau levels are still occupied (as is the case in the high field experiments on BEDT-TTF salts[2–5]).[15] The DOS therefore becomes

$$g[\varepsilon,B] = (D\Gamma/\pi)\sum_{n=1}^{\infty}([\varepsilon'(n)]^2+\Gamma^2)^{-1}, \tag{7}$$

where $D = NB/F \equiv 1/\pi b\lambda^2$ is the degeneracy of Landau levels, $\Gamma = \hbar/2\tau$ and $\lambda = \sqrt{\hbar/eB}$. For convenience, the energy variable has been changed via the transformation $\varepsilon' = \varepsilon - \hbar\omega_c(n-1/2) - W/2$, in order to shift the coordinates to the center of the Landau level.

As has been mentioned in Sec. I, in reality the Fermi surfaces of the α-phase BEDT-TTF salts consist of both Q2D and Q1D components,[9] each of which make their individual contributions, $g_{2D}[\varepsilon,B]$ and $g_{1D}[\varepsilon,B]$ respectively, to the DOS. These extra terms in the DOS can be included in the model by keeping the total number of electrons in the system constant whilst letting them distribute themselves amongst the Fermi surface components under the constraint that μ must be the same throughout. The Q1D part of the Fermi surface in the α-phase (BEDT-TTF) salts is an open orbit, and therefore does not undergo Landau quantization in the vicinity of μ. This part of the Fermi surface therefore behaves primarily as a carrier reservoir,[22] to and from which the carriers can flow in an attempt to minimize the free energy of the system. The size of this reservoir is determined by the total number of 1D states. In a truly 1D electron system, the DOS varies with energy as $1/\varepsilon$; however, in the context of this calculation it is only the DOS of the Q1D band in the vicinity of μ (the reservoir capacitance) which is important, and not the total number of 1D states. For the purpose of our calculations, we can therefore consider g_{1D} to be both independent of magnetic field and ε as a first approximation. The following summations are then valid:

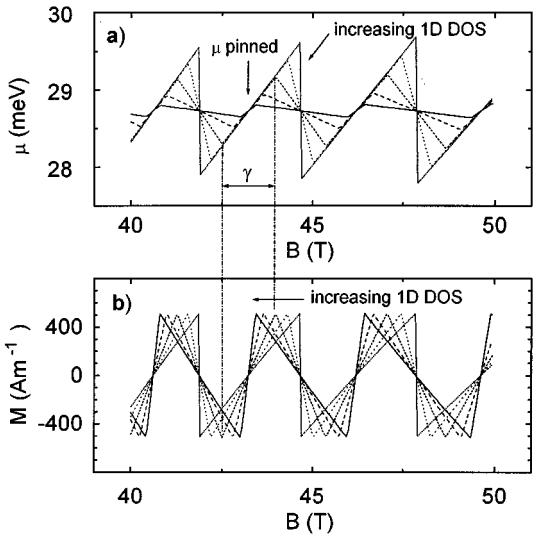

FIG. 1. (a) The calculated chemical potential for α-(BEDT-TTF)$_2$KHg(NCS)$_4$ where τ^{-1} and T are zero, for increasing values of $g_{1D}/\overline{g_{2D}}$ equal to 0, 1/3, 1, 3 and 10. This illustrates the effect of the presence of the additional DOS of the Q1D band on the wave form of the oscillations. (b) The corresponding magnetization. The interval γ (over which the chemical potential is pinned) is shown for the case when $g_{1D}/\overline{g_{2D}} = 1$ (note that the p-p amplitude of the magnetization is not affected by the presence of the Q1D band).

$$g[\varepsilon,B] = g_{1D} + g_{2D}[\varepsilon,B], \tag{8}$$

$$N = N_{1D} + N_{2D}. \tag{9}$$

In all the calculations, we have ignored the effects of Zeeman splitting of the Landau levels. In the experimental results which are considered, there is no evidence to suggest that spin splitting is a significant effect at high magnetic fields.[2–4]

Figure 1(a) shows the calculated chemical potential for various values of g_{1D} with τ^{-1} and T zero; the experimentally determined values $m^* = 2.7$ and $F = 670$ T, valid for α-(BEDT-TTF)$_2$KHg(NCS)$_4$ in its high field state[2] have been used. As would be expected, the oscillations of μ are largest when $g_{1D} = 0$, with a maximum possible peak-to-peak (p-p) amplitude equal to $\hbar\omega_c$. The fraction γ of the oscillation period over which μ increases with field corresponds to the situation where μ is pinned to the highest occupied Landau level. By increasing the relative contribution to the DOS coming from the Q1D component of the Fermi surface, both γ and the overall amplitude of the oscillations of μ become smaller. It can be shown that

$$\gamma = \frac{\overline{g_{2D}}}{g_{1D}+\overline{g_{2D}}}. \tag{10}$$

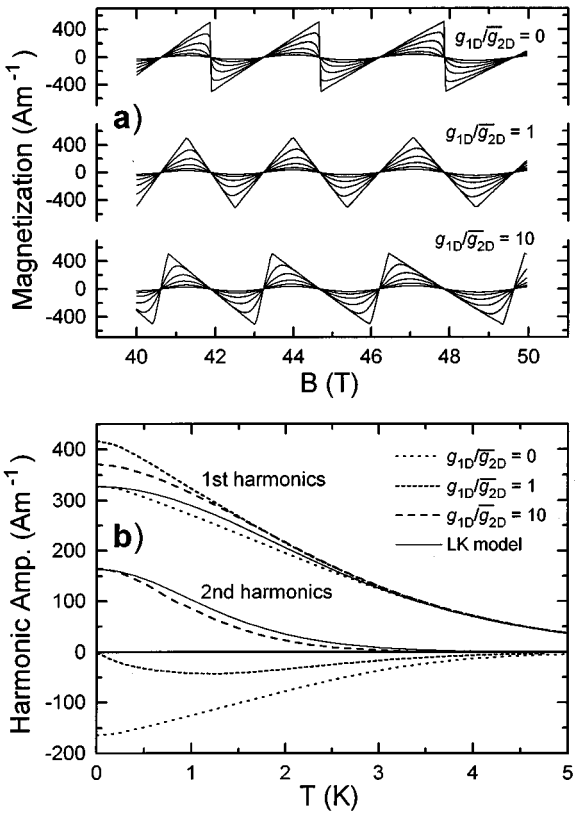

FIG. 2. (a) The magnetization calculated for different values of $g_{1D}/\overline{g}_{2D}$ (=0, 1 and 10) now at finite temperatures of T=0,1,2, . . . ,5 K. (b) A plot of the temperature dependence of the relative amplitudes of the fundamental and second harmonic contributions extracted by Fourier analysis. The relative harmonic amplitudes predicted by the 2D LK model are also shown for comparison.

The quantity γ also defines the fraction of the oscillation period over which the magnetization increases [as shown in Fig. 1(b)]. However, the absolute p-p amplitude of the magnetization is independent of g_{1D}. In the limit g_{1D}=0, the shape of the wave form corresponds to the ideal 2D limit, whilst as $g_{1D}\rightarrow\infty$, the wave form approaches that in the LK regime where $\mu\cong\varepsilon_F$, the Fermi energy.

Figure 2(a) shows a numerical calculation of the magnetization as a function of temperature for three different values of g_{1D} (see figure caption) and zero scattering rate. The temperature dependences of the amplitudes of the fundamental frequency and the second harmonic [Fig. 2(b)] differ markedly in the various cases considered. For ease of comparison, the temperature dependences of the fundamental frequency and second harmonic expected in the LK model have also been plotted. As the Fermi surface in question is Q2D, the 2D LK expression valid for a single slab of k space has been used, rather than the conventional 3D LK formula.[15] In the 2D LK approximation, the magnetization is

$$M=-a\sum_{p=1}^{\infty}R_p[T,B]\,\frac{1}{2\pi p}\,\sin\left[2\pi p\left(\frac{F}{B}-\frac{1}{2}\right)\right]e^{-\pi p/\omega_c\tau}, \tag{11}$$

where $R_p[T,B]=X_p/\sinh[X_p]$, $X_p=2\pi^2kTm_p^*/e\hbar B$, and $a=2e^2F/\pi bm^*$. Once again, the warping of the Fermi surface has been ignored and in Fig. 2(b), τ^{-1}=0. The total thickness of the Q2D Fermi surface slab in k space is equivalent to the reciprocal lattice parameter $2\pi/b$ perpendicular to the conducting planes. Note that in the term R_p, the masses $m_p^*=pm^*$; i.e., they are a factor p larger than the effective mass m^* of the fundamental frequency. As a result, the amplitudes of the higher harmonics in the LK theory are more strongly attenuated by increasing temperature than that of the fundamental frequency.[15]

Figure 2(b) shows that the second harmonic in the numerical calculations of the magnetization departs more strongly from the LK prediction. (The same is also true for the higher harmonics.) When $g_{1D}/\overline{g}_{2D}$=0, the second harmonic amplitude becomes negative due to the change in the left-right symmetry of the wave form [see Figure 1(a)]. In the case $g_{1D}/\overline{g}_{2D}$=1 (i.e., reservoir DOS equal to Q2D DOS), the wave form has no even harmonics at all when T=0 as it consists of a series of symmetrical triangles. Instead more spectral weight appears in the odd harmonics. Only when the temperature is increased do the even harmonics begin to appear; this tilting of the wave form at higher temperatures can be explained by the effective extension of the pinning interval γ as the temperature increases. When μ is situated directly between two neighboring Landau levels, the width of the Fermi-Dirac distribution has less influence on the magnetization at this point on the wave form, and hence it is less temperature dependent. When $g_{1D}/\overline{g}_{2D}$=10, the results of the numerical calculations correspond most closely to those of the LK theory. However, even in this case, the fundamental frequency has a slightly larger amplitude than that predicted by the LK theory due to a slight shifting of spectral weight from the even harmonics on to the odd harmonics.

In experimental studies, effective masses are often obtained by fitting the function $R_p=X_p/\sinh[X_p]$ (from 2D or 3D LK theory) to the various temperature dependences of the harmonic amplitudes of the quantum oscillations. If this process is carried out for magnetization amplitudes generated by the numerical calculations shown in Fig. 2(b), it is found that that $m_1^*\sim2.8$, $m_2^*\sim3.4$, and $m_3^*\sim3.8$ when $g_{1D}/\overline{g}_{2D}$=0. This now explains the origin of the low estimates of the effective masses obtained from the higher harmonics in dHvA measurements of α-(BEDT-TTF)$_2$KHg(NCS)$_4$ in its high field state.[2] Because the higher harmonics deviate strongly from the 2D LK theory and have a complicated temperature dependence, they cannot be used by themselves to determine the true effective mass.

The effects of Landau level broadening on the amplitude of the oscillations can also be investigated. A DOS which includes Landau level broadening was introduced in Eq. (7). Figure 3 shows the calculated magnetization for the two extreme cases, g_{1D}=0 and $g_{1D}\gg\overline{g}_{2D}$, at temperatures T=0 and T=2 K; the scattering rate has been set at $\tau^{-1}=0.5\times10^{12}$ s^{-1}, corresponding to a Dingle temperature of $T_D\sim0.6$ K.[15,19] Because μ oscillates with magnetic field, the damping factors of the oscillations for finite T and τ^{-1} can no longer be considered separately, but are interrelated. This renders the conventional ''Dingle analysis'' approach inappropriate.[15,19] Nevertheless, the fact remains that whether thermal damping, Landau level broadening or a

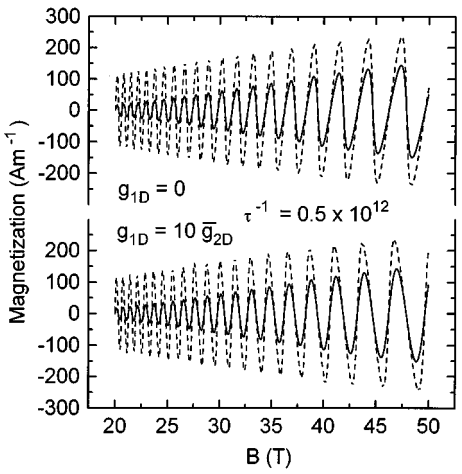

FIG. 3. The calculated magnetization for two different extreme cases of $g_{1D}/\overline{g_{2D}}$, to demonstrate the combined effects of a finite τ^{-1} and T. In the calculations we have used $\tau^{-1}=0.5\times10^{12}$ s^{-1}, and the temperatures 0 K and 2 K. The main observation is that although the shapes of the wave forms for the two cases differ somewhat at high magnetic fields, the peak to peak magnetization is independent of $g_{1D}/\overline{g_{2D}}$.

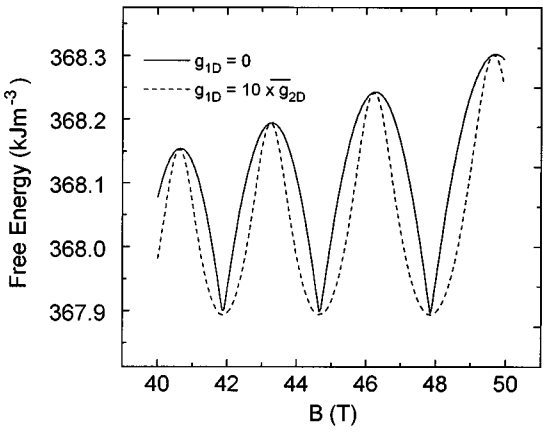

FIG. 4. The free energy F calculated for two different cases of $g_{1D}/\overline{g_{2D}}$. For the case where $g_{1D}/\overline{g_{2D}}=10$, the additional constant free energy contribution originating from the Q1D band has been subtracted in order to show that the peak to peak amplitudes are identical.

combination of the two is included, the p-p amplitude of the magnetization remains independent of g_{1D}. Only the shape of the wave form and hence the relative amplitudes of the harmonics are affected by the presence of additional Q1D states. This result can be understood by examining the analytical LK expression given as Eq. (11). The chemical potential appears only in the argument of the sine function, as $F/B=\mu/\hbar\omega_c$. In this way, an oscillatory $\mu[B,T,g_{1D}]$ will not affect the overall p-p amplitude of the oscillatory magnetization but just shift the relative positions of the minima and maxima in magnetic field.

A potentially useful empirical relationship can also be deduced from the results of the numerical calculations; for any g_{1D}, T or τ^{-1},

$$\tilde{M}\approx\frac{N}{\gamma B}\,\tilde{\mu} \tag{12}$$

(where $\tilde{M}$ and $\tilde{\mu}$ are the oscillatory components of the magnetization and chemical potential respectively) provided that $F/B>\sim10$.[23] A similar proportionality is thought to apply to 3D systems.[15] In that case, the quantity γ is defined approximately as $\overline{\tilde{g}}/\overline{g_{\rm tot}}$, where $\overline{g_{\rm tot}}$ refers to the field-averaged DOS of the entire Fermi surface.[15] Equation (12) is useful in that it enables approximate values of the magnetization to be calculated without calculating H_F. Alternatively for a given set of dHvA measurements it is possible to determine $\tilde{\mu}$ and hence the DOS.

IV. OBTAINING PARAMETERS FROM THE MAGNETIZATION

Experimental measurements of de Haas–van Alphen oscillations in the high field state of α-(BEDT-TTF)$_2$KHg(NCS)$_4$ show that at fields of $\sim$40 T both the Landau level broadening $\hbar\tau^{-1}=0.13$ meV ($T_D=0.25$ K) and the width of the Fermi-Dirac distribution function tail $kT=0.07$ meV are substantially less than the cyclotron energy $\hbar\omega_c=1.7$ meV.[2] The oscillations of μ are therefore expected to be significant in this material, and so it forms a useful test of the numerical calculations described in the previous sections.

The intermixing of the parameters T and τ^{-1} in Q2D systems, together with the absence of a general analytical expression for M, means that the simple analysis procedures which are appropriate for 3D systems can no longer be used. A point of departure is that the p-p magnetization amplitude is independent of the Q1D DOS. However, this does not turn out to be a very convenient approach for analyzing data, as the maxima and minima in M do not occur at fixed values of F/B (see, e.g., Figs. 1 and 2 where the positions clearly vary with both T and g_{1D}); before finding the p-p amplitude, any calculated expression for the magnetization must first be differentiated to locate the maxima and minima. The free energy H_F, on the other hand, also has a p-p amplitude which is independent of g_{1D} (an example of this is shown in Fig. 4) but possesses left-right symmetry (i.e., it is an even function). Hence its maxima occur at integer values of F/B and its minima occur at odd half-integer values of F/B (i.e., 1/2, 3/2, etc.). The p-p amplitude $H_{p\text{-}p}$ is independent of $g_{1D}(\varepsilon_F)$, because at the points where F/B is an even or odd half integer, μ is equal to the Fermi energy ε_F. Consequently, the p-p amplitude of the free energy is the same in the ideal 2D limit as it is for the 2D LK limit.

This latter observation provides a unique opportunity by which the amplitude of the oscillations can be interpreted in terms of the 2D LK result.[24] According to the 2D LK formula of Eq. (11), the p-p amplitude of the free energy is given by[15]

$$H_{p\text{-}p}\equiv 2\,\frac{B^2}{F}\sum_{p_{\rm odd}}\frac{M_p}{2\pi p}$$
$$=2a\,\frac{B^2}{F}\sum_{p_{\rm odd}}\frac{1}{4\pi^2p^2}\,\frac{X_p}{\sinh[X_p]}\,e^{-\pi p/\omega_c\tau}. \tag{13}$$

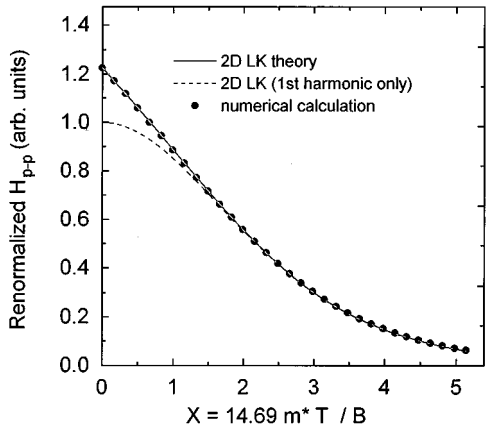

FIG. 5. The relative peak to peak amplitudes of the free energy calculated both from the 2D Lifshitz-Kosevich theory and the numerical calculations in the most extreme scenario when $g_{1D}/g_{2D}=0$. In addition we show the amplitude of the Lifshitz-Kosevich fundamental frequency by itself for comparison. All curves are renormalized so that the zero temperature amplitude of the latter curve is unity.

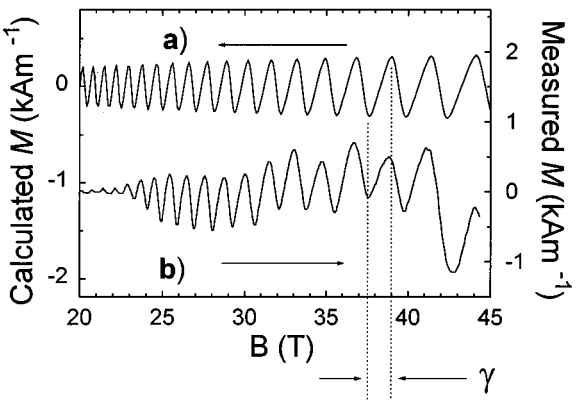

FIG. 6. (a) The numerically calculated magnetization using the parameters $m^*\tau^{-1}$ and g_{1D} which were determined experimentally in Ref. 2. (b) The corresponding measured magnetization. The arrows indicate the appropriate axes.

Here $H_p \cong B^2 M_p/2\pi pF$, and the M_p represent the Fourier components of the magnetization (note that the even coefficients do not contribute to $H_{p\text{-}p}$ and that care must be taken to use the correct sign of M_p). Equation (13) is plotted in Fig. 5 alongside the p-p amplitude obtained for the ideal 2D limit using the numerical calculations. The excellent agreement between the two methods demonstrates that Eq. (13) can be used with confidence to obtain m^* and T_D from measurements, even in the most extreme ideal 2D case.[24]

For many systems, the third or higher harmonic contributions to the experimental magnetization will be negligible. In α-(BEDT-TTF)$_2$KHg(NCS)$_4$, for example,[2] Fourier analysis of the dHvA signal in the high field state shows that the amplitude of the third harmonic is only approximately 8% of that of the fundamental. Since the dHvA signal is the second derivative of H_F, the magnitude of M_p/p in Eq. (13) for the third harmonic will in fact be nine times smaller than this. Therefore $M_3/3$ is $\sim$1% of $M_1/1$, and is on the threshold of being significant.

Including only the first and third harmonic terms of Eq. (13), we obtain

$$M_1+\frac{1}{3}M_3 = a\,\frac{X_1}{\sinh(X_1)}\,e^{-\pi/\omega_c\tau}+\frac{a}{9}\,\frac{X_3}{\sinh(X_3)}\,e^{-3\pi/\omega_c\tau}. \tag{14}$$

This formula can be iteratively fitted to the experimental values for M_p deduced for α-(BEDT-TTF)$_2$KHg(NCS)$_4$ at different temperatures[2] to yield an effective mass between 2.5 and 2.6 m_e, while the quasiparticle scattering rate τ^{-1} is approximately 0.2×10^{12} s^{-1}. The effective mass obtained should be compared with the value 2.7 m_e obtained in Ref. 2 by fitting the data to only $X_1/\sinh[X_1]$. Finally, g_{1D} is found by comparing numerical calculations of the magnetization with the experimental traces and adjusting g_{1D} to shift the maxima and minima in the numerical curves to the same positions as those in the experimental data. Such a procedure applied to the data of Ref. 2 requires the adjustment of only the parameter γ, yielding $g_{1D}/g_{2D}=0.4\pm0.2$.

To illustrate the results of this procedure. Fig. 6(a) shows a numerical calculation of the magnetization of α-(BEDT-TTF)$_2$KHg(NCS)$_4$ in its high field state using the parameters m^*, τ^{-1}, and g_{1D} determined from the data using the analysis procedure described above. Figure 6(b) shows the measured dHvA signal from Ref. 2, converted to magnetization by integration. A comparison of Figs. 6(a) and 6(b) suggests that the model is able to reproduce the features of the experimental data and provide a satisfactory estimate for the absolute amplitude of the magnetization. [The dramatic attenuation of the experimental oscillations seen in Fig. 6(b) below 25 T is due to the so-called ''kink'' field-induced phase transition, which is discussed in more detail in Ref. 2.]

V. THE OSCILLATORY MAGNETORESISTANCE

In contrast to the magnetization, the magnetoresistance cannot be directly related to the free energy, but instead depends on complicated scattering processes. It is therefore necessary for a number of approximations to be made in attempts to simulate experimental data. In high magnetic fields, it might naively be expected that the form of the Shubnikov–de Haas oscillations in organic Q2D systems would resemble those observed in 2D semiconductor systems such as Si inversion layers and GaAs-(Ga,Al)As heterostructures.[15,25] However, the magnetoresistance of 2D semiconductor systems is invariably measured with the current in the sample 2D plane. In contrast, measurements on the BEDT-TTF charge-transfer salts are typically made in the longitudinal direction, with the current parallel to the magnetic field and perpendicular to the Q2D conducting planes; this approach tends to avoid problems related to contact geometry and yields much larger (i.e., more easily measured) resistances.[10] For this reason, there are significant differences between the measurements made on organic conductors and those made on 2D semiconductor based systems.

Most theories of longitudinal magnetoresistance deal only with fully 3D systems,[26–28] as a strictly 2D system, by defi-

nition, has no conductivity perpendicular to the conducting plane. The organic conductors, therefore, represent an intermediate case between 2D and 3D extremes and have many properties in common with semiconductor superlattices.[29] Although in the above calculations of the Landau level density of states we have ignored the dispersion in the interplane direction, its existence must be reintroduced in order to calculate the longitudinal magnetoresistance. A useful starting point is formed by the model of Datars and Sipe,[29] developed for semiconductor superlattices; as will be seen below, the model provides an explanation for some of the essential features of the magnetoresistance oscillations observed in organic conductors[3,4] in spite of the fact that the relative energy scales are very different.

The component of the velocity in the longitudinal (interplane) direction in the Q2D organic conductors is very small compared to the typical values in 3D metals. Furthermore, although in 3D systems a large number of Landau levels contribute to the conductivity, a single Landau level dominates in Q2D systems at high magnetic fields. The latter point enables some approximations to be made, and therefore greatly simplifies the calculations. In the model of Datars and Sipe,[29] the longitudinal conductivity of the Q2D band is given by

$$\sigma_z = -e^2 \sum_n \frac{1}{2\pi^2 \lambda^2} \int \nu_z^2[n,k_z]\tau_t[\tilde{k}] f' dk_z , \qquad (15)$$

where f' is the derivative (with respect to ε) of the Fermi-Dirac distribution function. The longitudinal velocity $\nu_z = \partial\varepsilon/\hbar\partial k_z$ can be obtained from the dispersion relation of the Q2D band given by Eq. (1). In a magnetic field the dispersion relation becomes a series of Landau tubes of energy

$$\varepsilon_n = \hbar\omega_c\left(n - \frac{1}{2}\right) + \frac{W}{2}(1 - \cos[k_z b]). \qquad (16)$$

The quantity $\tau_t[\tilde{k}]$ is a transport scattering lifetime which depends on the transition rate between the initial and final k states (in Q2D systems it is often found to differ by a small numerical factor from the scattering time τ used in the calculation of Landau level widths[30]).

In order to calculate the conductivity, it is more convenient to integrate over ε rather than k_z; these two variables are related via the density of states

$$g[\varepsilon,B] = \frac{1}{\pi\lambda^2}\left(\frac{1}{\pi}\frac{\delta k_z}{\delta\varepsilon}\right). \qquad (17)$$

Although the transport scattering rate $1/\tau_t$ has a complicated dependence on k in the case of elastic scattering processes, it is generally thought to be proportional to the number of states into which the carriers can be scattered.[27,31] This is in turn proportional to the DOS; in accordance with this assumption, for isotropic scattering we consider the product $g[\varepsilon]\tau_t[\varepsilon]$ to be a constant. Using this approximation, it is therefore possible to define a constant state-averaged scattering rate $\overline{\tau_t} = \int \tau_t[\varepsilon] g[\varepsilon] d\varepsilon / \int g[\varepsilon] d\varepsilon \approx \tau_t g\varepsilon_F/N$. This approximate definition of a constant longitudinal transport scattering lifetime greatly simplifies the numerical calculations. Note, however, that the quasiparticle lifetime τ, which is responsible for the broadening of the Landau levels defined

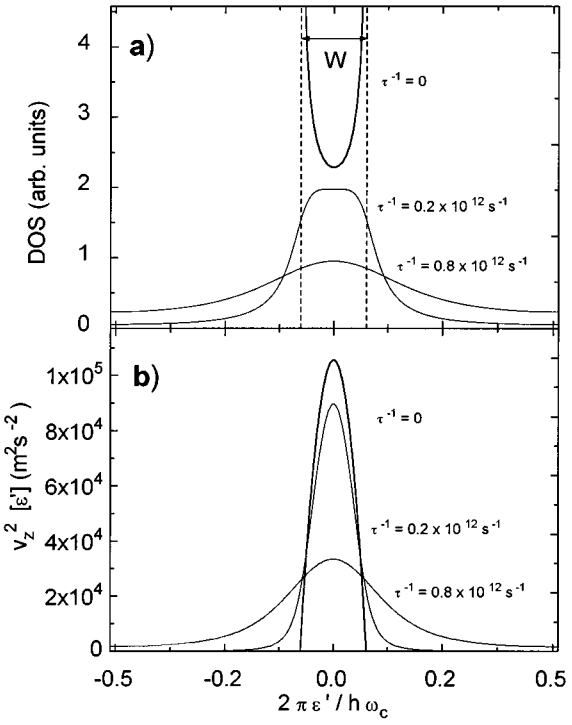

FIG. 7. (a) The thick line represents the density of states profile of the Landau level for a given minibandwidth (warping) in the absence of Landau level broadening. Additionally, as thin lines, we have calculated the Landau level broadening characteristic of the measured samples of α-(BEDT-TTF)$_2$KHg(NCS)$_4$ (Ref. 2) and in α-(BEDT-TTF)$_2$NH$_4$Hg(NCS)$_4$ (Ref. 3). (b) The statistical mean square velocity, with and without Landau level broadening included.

in Eq. (7), remains constant. Substituting the above and Eq. (16) and (17) into Eq. (15), we arrive at the conductivity

$$\sigma_z \cong -\frac{1}{2} e^2 \frac{N}{\varepsilon_F} \sum_n \overline{\tau_t} \int \nu_z^2[n,k_z] f' d\varepsilon . \qquad (18)$$

In the absence of Landau level broadening effects, each k-state can be associated with a single eigenstate energy. Expressing the velocity as a function of energy then enables a straightforward numerical calculation of the conductivity to be carried out.

The uppermost curves (drawn in thicker lines to represent the situation where $\tau^{-1}=0$) in Figs. 7(a) and 7(b) show the profile of the DOS $g[\varepsilon']$ and the square velocity $\nu_z^2[\varepsilon']$. For the purpose of these calculations we have assumed that $B=50$ T and $m^*=3m_e$ and the ratio $\Delta F/F$ has been taken to be ~ 0.01; this latter quantity is only an upper limit which is thought to be consistent with recent experimental observations.[12,14] The DOS profile in Fig. 7(a) exhibits two singularities which correspond to the top and bottom of the band. Although the group velocity of the quasiparticles within the conducting planes is $\sim 10^4$ ms^{-1}, the component of velocity in the longitudinal direction is more than one order of magnitude lower, reflecting the small dispersion in that direction. When the chemical potential is situated at the top or bottom of the band, the longitudinal component of velocity is zero [see Fig. 7(b)]. In principle, the conductivity

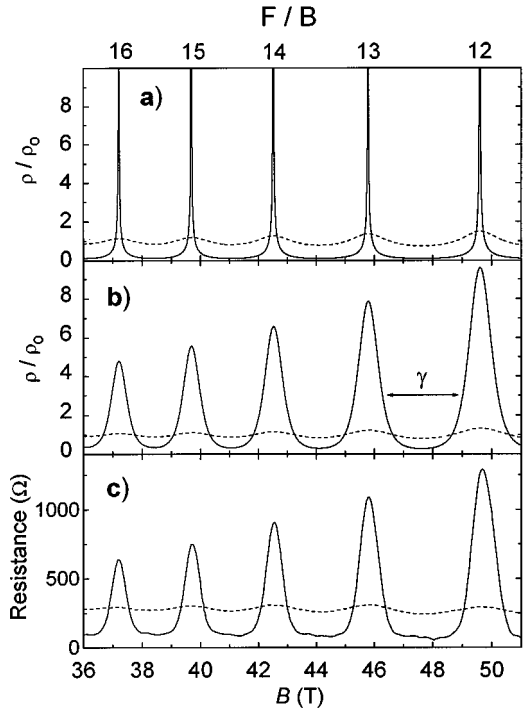

FIG. 8. (a) The calculated magnetoresistance for in α-(BEDT-TTF)$_2$NH$_4$Hg(NCS)$_4$ assuming the model of Datars and Sipe (Ref. 29) for $T=0.4$ K (solid line) and $T=4$ K (dashed line). (b) The calculated magnetoresistance including the Landau level broadening according to the Dingle temperature estimated by Sandhu *et al.* (Ref. 3). The approximate interval γ over which the chemical potential is pinned to a Landau level is also indicated. (c) The corresponding measured magnetoresistance for α-(BEDT-TTF)$_2$NH$_4$Hg(NCS)$_4$ of Sandhu *et al.* (Ref. 3).

should also be zero at this point, but for practical reasons this can never be realized, due to the effects of finite temperature and Landau level broadening. Nevertheless, at integer values of F/B, we should expect a minimum in the conductivity and hence a maximum in magnetoresistance. This is precisely what is observed in the organic conductor α-(BEDT-TTF)$_2$NH$_4$Hg(NCS)$_4$ (Ref. 3) [reproduced in Fig. 8(c)] and in semiconductor superlattices.[32] In contrast, the transverse magnetoresistance of 2D semiconductor based systems exhibits a minimum in magnetoresistance at integer values of F/B.[25]

Figure 8(a) shows a calculation of the longitudinal magnetoresistance $\rho_z=1/\sigma_z$ for α-(BEDT-TTF)$_2$NH$_4$Hg(NCS)$_4$ carried out using Eq. (18). The parameters $F=595$ T (Ref. 33) and $m^*=3m_e$ taken from Ref. 3 have been used; the two curves represent $T=0.4$ and 4 K. In addition, τ^{-1} has been set to zero, as in the upper curves in Fig. 7(a) and 7(b). Consequently, very sharp magnetoresistance maxima are observed (particularly for $T=0.4$ K) as might be expected in a sample with no scattering.

In order to provide a more realistic simulation of the data, the effects of scattering must be taken into account. In many papers, Landau level broadening is often ignored in the derivation of a formula for the SdH effect, and is only inserted in the final solution as a Dingle reduction factor.[19,26,27] The latter approach is somewhat unsatisfactory and in the present calculation the effects of broadening are included in a similar manner to the quantum mechanical derivation of Kubo *et al.*,[28] by considering the Lorentzian distribution function

$$s[\varepsilon]=\frac{\Gamma}{(\varepsilon_n-\varepsilon)^2+\Gamma^2}; \tag{19}$$

renormalized such that $\int_{-\infty}^{\infty}\hbar s^2[\varepsilon]/\pi d\varepsilon=\tau$. Equation (18) can then be rewritten as

$$\sigma_z=-\frac{1}{2}e^2\frac{N}{\varepsilon_F}\sum_n\int\frac{\hbar\tilde{\tau}_t}{\pi\tau}\langle s^2[\varepsilon]\nu_z^2[n,k_z]\rangle_{k_z}f'd\varepsilon, \tag{20}$$

where the triangular brackets represent an ensemble average over all possible k_z states. The function $s[\varepsilon]$ is counted twice in this expression, since both the initial and final states involved in the scattering process are broadened. By taking the limit as Γ tends to zero, $s[\varepsilon]$ approaches a δ function, and Eq. (20) reduces back to Eq. (18). In contrast to the theoretical calculations of Kubo *et al.*, in the present model we have ignored any possible shift of the energy states and have assumed Γ to be independent of ε in order to be consistent with our DOS defined by Eq. (7). The average over k_z in the model reduces to the convolution $\nu_z^2*s^2[\varepsilon]$, resulting in the definition of a broadened square velocity $\overline{\nu_z^2}[\varepsilon']$. This is shown together with the broadened DOS in Figs. 7(a) and 7(b); the curves are calculated using the measured quasiparticle scattering rates for α-(BEDT-TTF)$_2$KHg(NCS)$_4$ (Ref. 2) and α-(BEDT-TTF)$_2$NH$_4$Hg(NCS)$_4$.[3] Figure 7(a) clearly indicates that the double-peaked structure of the DOS can no longer be clearly resolved, especially in the case of the latter salt; this point justifies ignoring the warping of the Fermi surface for the purpose of the magnetization calculations.

Note that a potentially useful further approximation can be made in the limit $W\ll\Gamma$, which appears to apply to the experiments on α-(BEDT-TTF)$_2$NH$_4$Hg(NCS)$_4$ in Ref. 3. In this case, the detailed k_z dependence of the velocity is no longer important, and the broadened square velocity is given approximately by $\overline{\nu_z^2}[\varepsilon']\propto s^2[\varepsilon]$. Furthermore, in this extreme limit, the structure in the DOS arising from the dispersed band is of little importance and the DOS is $g_{2D}[\varepsilon,B]\propto\Sigma_n s[\varepsilon]$. With $g_{2D}=\tilde{g}_{2D}+\overline{g_{2D}}$, the contribution to the conductivity from the Q2D portion of the Fermi surface can then be approximated by

$$\sigma_{2D}\approx\sigma_{2D,0}\int_0^\infty\left(1+2\frac{\tilde{g}_{2D}[\varepsilon,B]}{\overline{g_{2D}}}+\frac{\tilde{g}_{2D}^2[\varepsilon,B]}{\overline{g_{2D}^2}}\right)f'[\varepsilon]d\varepsilon, \tag{21}$$

where the background (zero field) conductivity $\sigma_{2D,0}[0]=e^2N\tau_tW/\pi m_z\varepsilon_F$ can be found by taking the limit of Eq. (20) as $\Gamma\to\infty$, and where m_z is the average mass of the band in the k_z direction. Finally, the contribution to the conductivity from the Q1D band can also be included by summing the various components so that the total conductivity is given by $\sigma=\sigma_{2D}+\sigma_{1D}$.

Figure 8(b) shows the magnetoresistance calculated for the temperatures $T=0.4$ and 4 K predicted by Eq. (20) using the value $\tau^{-1}=0.8\times10^{12}$ s^{-1} deduced for α-(BEDT-TTF)$_2$NH$_4$Hg(NCS)$_4$ in Ref. 3, assuming that $g_{1D}/\overline{g_{2D}}\sim0.4$ [as for α-(BEDT-TTF)$_2$KHg(NCS)$_4$], and ig-

noring the conductivity contribution from the Q1D portion of the Fermi surface. (Note, however that the ratio $g_{1D}/\overline{g_{2D}}$ has been used to calculate μ in the Fermi-Dirac distribution function.) The curve calculated from Eq. (20) is indistinguishable from one calculated using the more approximate Eq. (21), indicating that the latter simplified procedure may be used with confidence in the case of α-(BEDT-TTF)$_2$NH$_4$Hg(NCS)$_4$ in high magnetic fields.

The calculated longitudinal magnetoresistance in Fig. 8(b) shows a good resemblance to the data measured in Ref. 3, which are shown for comparison in Fig. 8(c); these are qualitatively similar to the data published in Ref. 4 for the selenium-based salts which are thought to have similar material parameters. The extent to which the Q1D band contributes to the longitudinal conductivity is not known, as the Fermi surface warpings of the Q1D and Q2D components have not yet been measured. Needless to say, there are considerable differences between the Q2D and Q1D bands; while the Q2D energy band experiences Landau level quantization and therefore intersects with the chemical potential at a single point, the Q1D band is not Landau quantized, and therefore intersects the chemical potential for all values of k_z. For this reason, one might expect the nature of the scattering to be different for the two bands. The similarity of Fig. 8(b) to the experimental data of Fig. 8(c) suggests that the contribution of the Q1D band to the longitudinal conductivity is practically negligible.

The effect of introducing a small and constant contribution to the conductivity will be both to lower and to round off the peaks in the magnetoresistance. However, qualitatively the greatest effect of the presence of the Q1D band results from the effect of its DOS on μ, which alters the width of the magnetoresistance maxima; the width of the shallow region between maxima roughly corresponds to the interval γ over which μ is pinned. A comparison of the model [Fig. 8(b)] and the data [Fig. 8(c)] therefore suggests that the DOS of the Q1D component of the Fermi surface may be somewhat less in α-(BEDT-TTF)$_2$NH$_4$Hg(NCS)$_4$ than for α-(BEDT-TTF)$_2$KHg(NCS)$_4$. However, given the approximations in deriving the model, it would be unwise to make any quantitative estimates on the basis of this comparison.

One of the most striking observations from experimental magnetoresistance studies has been the ''apparent'' increase of the effective mass at high magnetic fields.[3,4] In order to make a more direct comparison of the above model with experiment, in Fig. 9 (filled square symbols) we have applied conventional LK analysis by fitting the function $R_p = X_p/\sinh[X_p]$ to the temperature dependence of the calculated SdH oscillations; an example of a calculated trace at 0.4 K is shown as an inset. For comparison, we have also determined the apparent effective masses for the calculated magnetization (using the same material parameters valid for α-(BEDT-TTF)$_2$NH$_4$Hg(NCS)$_4$). It is evident from Fig. 9 that the apparent effective masses determined from the calculated magnetoresistance increase steadily with increasing magnetic field, in a manner qualitatively similar to experimental observations.[3,4] In contrast, as discussed in Secs. III and IV the apparent effective mass associated with the fundamental frequency of the magnetization is only slightly increased.

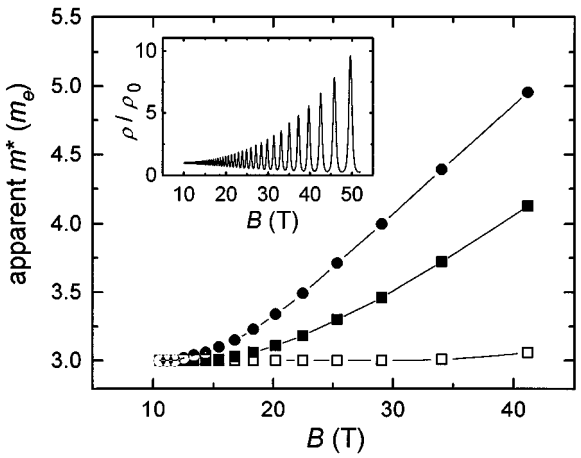

FIG. 9. The apparent effective masses versus magnetic field obtained by fitting the LK temperature reduction factor R_T to the calculated magnetoresistance (filled squares) and the calculated magnetization (open squares) for α-(BEDT-TTF)$_2$NH$_4$Hg(NCS)$_4$. To illustrate that the apparent effective mass is sensitive to other parameters such as the scattering rate, we have also plotted the apparent effective mass for the identical system but with τ^{-1} reduced by 25% (filled circles). The inset shows an example of a calculated magnetoresistance trace at 0.4 K.

Since the value $m^*=3$ was used in the model calculations, we can therefore conclude that the apparent increase in effective mass reflects the failure of the conventional LK theory to describe the form of the temperature dependence of the oscillations at high magnetic fields, and cannot be interpreted as a real increase of the effective mass. This apparent effective mass depends not only on magnetic field, but also on the degree of Landau level broadening. To illustrate this point, in Fig. 9 (circle symbols) we have also calculated the apparent effective mass for the same material parameters, but with the scattering rate reduced by 25%.

A higher apparent effective mass indicates that the oscillations have a much stronger temperature dependence than predicted by the LK theory. To further illuminate this point, Fig. 10(a) shows the actual temperature dependence of the amplitude of the fundamental frequency of the numerically calculated magnetoresistivity [determined over the field interval shown in Fig. 8(b)]. For comparison, Fig. 10(a) also includes the amplitude according to the LK prediction. The numerically calculated amplitude has been renormalized to that of the LK prediction at higher temperatures, where the two agree. [Such agreement is not unexpected; from Eq. (21) it is evident that at low magnetic fields $\tilde{g}_{2D}/\overline{g_{2D}} \ll 1$]. From Fig. 10(a), it is clear that the additional temperature dependence responsible for the ''enhanced'' effective mass occurs at the lower temperatures, and is due to a strong increase in the magnetoresistance peaks. This effect is unique to the longitudinal magnetoresistance owing to the fact that it becomes divergent when the chemical potential is situated in (or close to) the gap between adjacent Landau levels.

Finally, Fig. 10(b) compares the calculated p-p magnetoresistance ρ_{p-p}/ρ_0 and the measured p-p magnetoresistance of Ref. 3. The close agreement between the two illustrates that Eqs. (20) and (21) provide a good approximation for the behavior of the magnetoresistance of α-phase BEDT-TTF salts. There exists, however, a scaling factor between

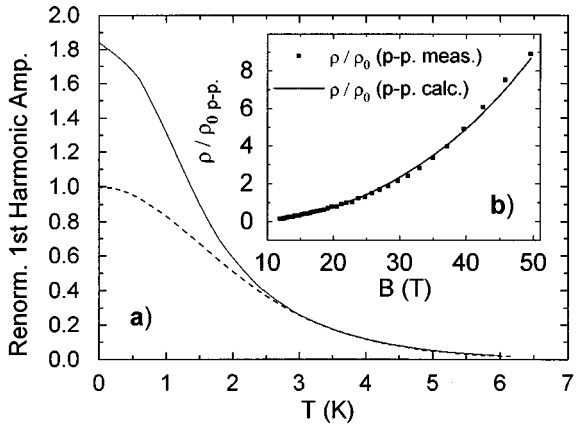

FIG. 10. (a) The amplitude of the fundamental frequency versus temperature, calculated according to our model for the magnetoresistance (solid line). This is compared with that expected assuming the Lifshitz-Kosevich theory (dashed lines). At high temperatures, the calculated amplitude has been renormalized to that of the Lifshitz-Kosevich theory. This indicates the strong increase of the oscillatory magnetoresistance at low temperatures. (b) A comparison between the measured (Ref. 3) and calculated peak-to-peak amplitude of the oscillatory magnetoresistance as a function of magnetic field.

measured and calculated values of ρ_{p-p}/ρ_0, which may be due to additional series resistances or voltages contributing to the measured signal. Additional nonoscillatory series resistances could, for example, originate from layers of the sample which are damaged or have a higher impurity content.

VI. SUMMARY

Using a combination of numerical methods and simple physical models, we have been able to account for the departures from conventional LK behavior which have been observed recently in the quantum oscillations of organic conductors in high magnetic fields. The calculations are based on the thermodynamics of an ideal 2D electron gas, which is found to be appropriate at high magnetic fields ($B>20$ T). The advantage of the numerical calculations is that both the effects of finite temperature and Landau level broadening can be correctly included, which has so far not been possible in analytical calculations. The effect of the pinning of the chemical potential to the Landau levels is found to have a dramatic effect on the sign and temperature dependence of the harmonics of the magnetization oscillations, and provides an explanation for the apparent low effective masses which have been observed for the harmonics in the high field state of α-(BEDT-TTF)$_2$KHg(NCS)$_4$.[2] Furthermore, the presence of additional states in the Q1D portion of Fermi surface is found to have a pronounced influence on the wave form of the oscillations. Comparison of the numerical calculations with real measurements[2] provides an opportunity to estimate the DOS associated with the Q1D portion of Fermi surface, which otherwise could not be measured.

A further result which emerges from the analysis is that whilst the wave form of the oscillations is significantly perturbed by the effects of an oscillatory chemical potential, the peak to peak amplitude of the free energy is independent of this, and also therefore independent of the size of the DOS of the Q1D portion of the Fermi surface. This provides a procedure by which the true effective mass and quasiparticle scattering rates can be extracted from experimental data, even in extreme 2D systems in high magnetic fields.

The main features of the longitudinal magnetoresistance in quasi-two-dimensional organic conductors at high magnetic fields can be understood in terms of theories for the conductivity which are normally applicable to semiconductor superlattices.[29] In particular, the strongly peaked (or divergent) behavior of the magnetoresistance oscillations at high magnetic fields and low temperatures are due to the chemical potential lying in (or close to) the gap between two adjacent Landau levels. The relatively short interval (in $1/B$-space) over which the chemical potential is situated in (or close to) the gap is responsible for the sharpness of the oscillation maxima. We believe that it is this effect which is responsible for the anomalously high apparent effective masses which have been observed in recent magnetoresistance measurements on the α-phase organic conductors in high magnetic fields.[3,4]

Note added in proof. After going to press we learned of de Haas–van Alphen measurements carried out on θ-(BEDT-TTF)$_2$I$_3$ in magnetic fields of up to 25 T.[34,35] The Fermi surface of this material consists solely of a quasi-two-dimensional cylinder and the samples studied have very long scattering times. Consequently, the de Haas–van Alphen oscillations appear as a series of very sharp ''saw teeth,'' satisfying similar to the predictions of the numerical calculations shown in the upper part of Fig. 3 ($g_{1D}=0$). We thank Professor M. Tokumoto for pointing out these experimental data.

ACKNOWLEDGMENTS

We would like to thank Professor David Shoenberg for illuminating discussions. We would also like to thank Professor James Brooks and Pavi Sandhu for providing data prior to publication. This work has received financial support from the EPSRC, the Royal Society (UK) and Belgium National Science Foundation, and N.H. and P.H.P.R. are supported by the Onderzoeksraad, KU Leuven. J.S. would like to acknowledge financial support at KU Leuven which initiated the high field studies on these materials.

[1] I. M. Lifshitz and A. M. Kosevich, Zh. Éksp. Teor. Fiz. **29**, 730 (1956).

[2] N. Harrison, A. House, I. Deckers, J. Singleton, F. Herlach, W. Hayes, M. Kurmoo, and P. Day, Phys. Rev. B **52**, 5584 (1995).

[3] P. S. Sandhu, G. J. Athas, J. S. Brooks, E. G. Haanappel, J. D. Goettee, D. W. Rickel, M. Tokumoto, N. Kinoshita, T. Kinoshita, and Y. Tanaka, Surf. Sci. **361-362**, 913 (1996).

[4] V. N. Laukhin, A. Audouard, H. Rakoto, J. M. Broto, F. Goze, G. Coffe, L. Brossard, J. P. Redoules, M. V. Kartsovnik, N. D. Kushch, L. I. Buravov, A. G. Khomenko, E. B. Yagubskii, S.

Askenazy, and P. Pari, Physica B **211**, 282 (1995).

[5] E. Balthes, D. Schweitzer, I. Heinen, H. J. Keller, W. Strunz, W. Biberacher, A. G. M. Jansen, and E. Steep, Z. Phys. B **99**, 163 (1995).

[6] See, for example, X. D. Shi, W. Kang, and P. M. Chaikin, Phys. Rev. B **50**, 1984 (1994) and references therein.

[7] J. S. Brooks, X. Chen, S. J. Klepper, S. Valfells, G. J. Athas, Y. Tanaka, T. Kinoshita, N. Kinoshita, M. Tokumoto, H. Anzai, and C. C. Agosta, Phys. Rev. B **52**, 14 457 (1995); S. Uji, T. Terashima, H. Aoki, J. S. Brooks, M. Tokumoto, N. Kinoshita, T. Kinoshita, Y. Tanaka, and H. Anzai, J. Phys. Condens. Matter **6**, L539 (1994); S. Uji, H. Aoki, J. S. Brooks, A. S. Perel, G. J. Athas, S. J. Klepper, C. C. Agosta, D. A. Howe, M. Tokumoto, N. Kinoshita, Y. Tanaka, and H. Anzai, Solid State Commun. **88**, 683 (1993).

[8] J. Caulfield, S. J. Blundell, M. S. L. du Croo de Jongh, P. T. J. Hendriks, J. Singleton, M. Doporto, F. L. Pratt, A. House, J. A. A. J. Perenboom, W. Hayes, M. Kurmoo, and P. Day, Phys. Rev. B **51**, 8325 (1995).

[9] H. Mori, S. Tanaka, M. Oshima, G. Saito, T. Mori, Y. Maruyama, and H. Inokuchi, Bull. Chem. Soc. Jpn. **63**, 2183 (1990).

[10] J. Wosnitza, Int. J. Mod. Phys. **7**, 2707 (1993); M. Tokumoto, A. G. Swanson, J. S. Brooks, C. C. Agosta, S. T. Hannahs, N. Kinoshita, H. Anzai, M. Tamura, H. Tajima, H. Kuroda, and J. R. Anderson, in *Organic Superconductivity*, edited by V. Z. Krezin and W. A. Little (Plenum, New York, 1990).

[11] W. Kang, G. Montambaux, J. R. Cooper, D. Jérome, P. Batail, and C. Lenoir, Phys. Rev. Lett. **62**, 2559 (1989).

[12] Recently Haworth *et al.* in Ref. 14 have tentatively proposed the existence of beating effects at low magnetic fields in α-(BEDT-TTF)$_2$KHg(SCN)$_4$, although it is not yet known for certain whether this can be genuinely related to the Fermi surface geometry or whether it is an artifect of the SDW ground state or measurement technique.

[13] M. V. Kartsovnik, H. Ito, T. Ishiguro, H. Mori, T. Mori, G. Saito, and S. Tanaka, J. Phys. Condens. Matter **6**, L479 (1994).

[14] C. Haworth, J. Caulfield, A. House, J. Singleton, M. Springford, P. Meeson, M. Kurmoo, P. Day, and W. Hayes (unpublished); C. Haworth, Ph.D. thesis, University of Bristol, 1995.

[15] D. Shoenberg, *Magnetic Oscillations in Metals* (Cambridge University Press, Cambridge, 1984).

[16] I. D. Vagner, Tsofar Maniv, and E. Ehrenfreund, Phys. Rev. Lett. **51**, 1700 (1983).

[17] See, for example, K. Jauregui, V. I. Marchenko, and I. D. Vagner, Phys. Rev. B **41**, 12 922 (1990) and references therein.

[18] K. Jauregui, W. Joss, V. I. Marchenko, S. V. Meshkov, and I. D. Vagner, in *High Magnetic Fields in Semiconductor Physics III*, edited by H. K. V. Lotsch, Springer Series in Solid-State Sciences 101 (Springer-Verlag, Berlin, 1992), p. 668.

[19] R. B. Dingle, Proc. R. Soc. London Ser. A **211**, 500 (1952).

[20] A. Potts, R. Shepherd, W. G. Herrendon-Harker, M. Elliott, C. L. Jones, A. Usher, G. A. C. Jones, D. A. Ritchie, E. H. Linfield, and M. Grimshaw, J. Phys. Condens. Matter **8**, 5189 (1996).

[21] N. W. Ashcroft and N. D. Mermin, *Solid State Physics* (Holt, Rinehart and Winston, Philadelphia, 1976), p. 53.

[22] An analytical approach including the existence of an additional reservoir of carriers was developed by I. D. Vagner, T. Maniv, W. Joss, J. M. van Ruitenbeek, and K. Jauregui, Synth. Met. **34**, 393 (1989).

[23] This result can be understood using the following argument. At $T=0$ and for $g_{1D}=0$, the energy of n filled Landau levels is $\Sigma_{m=1}^{n}(m+1/2)(N/n)\hbar\omega_c$ which is constant when NB is constant; hence $\partial N/\partial B|_{H_F}=-N/B$. Using the identity $\partial H_F/\partial B|_{N,T}=-\partial H_F/\partial N|_{B,T}\cdot\partial N/\partial B|_{H_F,T}$ we have $\tilde{M}=\tilde{\mu}N/B$. This will hold for $T>0$ as the phase smearing equally affects $\tilde{\mu}$ and $\tilde{M}$. When $g_{1D}>0$, the peak-to-peak amplitude of $\tilde{M}$ is unchanged (as discussed in the text) but the effect on $\tilde{\mu}$ is partially ''bypassed'' by the capacity of the 1D reservoir and therefore reduced by a factor γ; thus Eq. (12).

[24] The 2D LK model is calculated using the Poisson summation rule, which is only valid when μ is assumed to be constant and when $F/B\gg 1$ (see Appendix 3 of Ref. 15).

[25] See, for example, T. Ando, A. B. Fowler, and F. Stern, Rev. Mod. Phys. **54**, 437 (1982).

[26] P. N. Argyres, J. Phys. Chem. Solids **4**, 19 (1958).

[27] L. M. Roth and P. N. Argyres, *Semiconductors and Semimetals* (Academic, New York, 1966), Vol. 1, p. 159.

[28] R. Kubo, S. J. Miyake, and N. Hashitsume, in *Solid State Physics*, edited by F. Seitz and D. Turnbell (Academic, New York, 1965), Vol. 17, p. 269.

[29] A. E. Datars and J. E. Sipe. Phys. Rev. B **51**, 4312 (1995).

[30] J. P. Harrang, R. J. Higgins, R. K. Goodall, P. R. Jay, M. Laviron, and P. Delescluse, Phys. Rev. B **32**, 8126 (1985); P. T. Coleridge, R. Stoner, and R. Fletcher, *ibid*. **39**, 1120 (1989); A. Gold, *ibid*. **38**, 10 798 (1988).

[31] A. B. Pippard, *The Dynamics of Conduction Electrons* (Blackie and Son, Glasgow, 1965).

[32] H. Noguchi, H. Sakaki, T. Takamasu, and N. Miura, Physica B **184**, 293 (1993).

[33] The value of $F=595$ T is somewhat different from the value of 570 T which is normally quoted (Refs. 8–10). This difference appears to suggest that the **b** axis of the sample was rotated to an angle of approximately 17° with respect to the direction of the magnetic field.

[34] M. Tokumoto, A. G. Swanson, J. S. Brooks, M. Tamura, H. Tajima, and H. Kuroda, Solid State Commun. **75**, 439 (1990).

[35] M. Tokumoto, A. G. Swanson, J. S. Brooks, C. C. Agosta, S. T. Hannahs, N. Kinoshita, H. Anzai, M. Tamura, H. Tajima, H. Kuroda, A. Ugawa, and K. Yakushi, Physica B **184**, 508 (1993).